Available online at www.sciencedirect.com
ScienceDirect
Ceramics International 34 (2008) 365–370
CERAMICS INTERNATIONAL
www.elsevier.com/locate/ceramint

Phase stability, microstructural evolution and room temperature mechanical properties of TiO_2 doped 8 mol% Y_2O_3 stabilized ZrO_2 (8Y-CSZ)

Tiandan Chen [a], Süleyman Tekeli [b,*], Robert P. Dillon [a], Martha L. Mecartney [a]

[a] Department of Chemical Engineering and Materials Science, University of California, Irvine, CA 92697-2575, USA
[b] Materials Division, Technical Education Faculty, Gazi University, 06500, Besevler-Ankara, Turkey

Received 26 July 2006; received in revised form 20 September 2006; accepted 22 October 2006
Available online 14 December 2006

Abstract

The effect of TiO_2 dopant on phase stability, microstructural evolution and room temperature mechanical properties of 8 mol% yttria-stabilized cubic zirconia (8Y-CSZ) was studied. The results show that TiO_2 (up to 10 wt%) can be dissolved in solid solution in the zirconia matrix. When the dopant amount is less than 5 wt%, TiO_2 doped 8Y-CSZ remains single phase cubic zirconia. Increased additions of TiO_2 destabilize the cubic phase and cause the formation of tetragonal zirconia with a resultant microstructure consisting of large cubic zirconia grains and small tetragonal zirconia grains. EDS analyses show that yttria is partitioned between these two types of grains. The solubility of TiO_2 is the highest for cubic grains which also have higher yttria concentrations. Room temperature mechanical property measurements show that hardness does not change significantly with additions of TiO_2, but fracture toughness is more than doubled for 10 wt% TiO_2 doped 8Y-CSZ.

Keywords: Cubic zirconia; TiO_2 dopant; Phase evolution and microstructure; Hardness and fracture toughness

1. Introduction

Zirconia exists in three different crystal structures: monoclinic, tetragonal and cubic. The fluorite cubic structure of zirconia can be stabilized at room temperature by the addition of Y_2O_3 in solid solution (YSZ). Cubic YSZ is used as a solid electrolyte in solid oxide fuel cells (SOFC) due to its excellent stability and high oxygen ionic conductivity over wide range of temperatures and oxygen partial pressure [1], and also for thermal barrier coatings (TBC) because of its low thermal conductivity and good erosion resistance [2]. However, cubic zirconia has modest mechanical properties. For both SOFC and TBC applications, good mechanical and chemical stability are desired in order to prevent fracture due to thermal and mechanical stresses during use [2,3]. Therefore, the enhancement of mechanical properties for cubic zirconia is desired.

To improve the mechanical properties of YSZ, different additives including SiO_2 [4], Al_2O_3 [5–7] and SiC [8] have been used. However, SiO_2, Al_2O_3 and SiC form insulating second phases and may also cause degradation of ionic conductivity. Other dopants that can improve the mechanical properties and maintain the conductivity of cubic zirconia are worth being explored further. TiO_2 has been proposed as an effective additive [9]. The Ti^{4+} ion is tetravalent as is Zr^{4+} with a slightly smaller ion size, i.e., 0.068 nm for Ti^{4+} and 0.079 nm for Zr^{4+}. The solubility of TiO_2 in tetragonal zirconia [10] and cubic zirconia [11] at 1400 °C is as high as 15 mol%. In addition, TiO_2 doped cubic zirconia should have excellent stability at high temperatures and good compatibility with the YSZ electrolytes and Ni-based alloys [12]. The addition of TiO_2 to YSZ under reducing conditions increases the electronic conductivity and grain boundary ionic conductivity [13]. Although the conductivity of TiO_2 doped YCSZ has been studied, there are few reports about the mechanical behavior in the literature. In this current work, the phase, microstructural evolution and the room temperature mechanical properties of different amounts of TiO_2 doped 8Y-CSZ were studied.

2. Experimental procedure

Starting powders were nanoscale 8 mol% yttria stabilized cubic zirconia (TOSOH, Japan) and high-purity TiO_2 (Rare

* Corresponding author. Tel.: +90 312 4399760; fax: +90 312 2120059.
E-mail address: stekeli@gazi.edu.tr (S. Tekeli).

0272-8842/$34.00
doi:10.1016/j.ceramint.2006.10.015

Metallic, Japan) powders. 8Y-CSZ powders were doped by adding different amounts of TiO_2 (up to 10 wt%) and then ball-milling in ethanol for 24 h by using zirconia balls. The as-prepared slurries were dried in air and then die-pressed into disks by uniaxial pressing at 40 MPa in a steel die followed by cold isostatic pressing at 100 MPa. The green compacts of the mixed powders were sintered at 1450 °C for an hour in air. The densities of as-sintered samples were measured using the Archimedes method in distilled water.

The microstructure of as-sintered samples was investigated using scanning electron microscopy (SEM) (Philips XL 30FEG) and transmission electron microscopy (TEM) (Philips CM20). Grain sizes were determined from the SEM micrographs using Scionimage software. The 3D grain size was determined to be 1.56L, where L is the average 2D grain size measured from SEM images. TEM foils were prepared using conventional way, dimple polishing on one side, and ion beam thinning of both sides to electron transparency. X-ray diffraction patterns (XRD) of the samples were obtained using a Siemens D-5000 Diffractometer and monochromated high intensity Cu Kα radiation. A scan speed of 0.02 $2\theta\ s^{-1}$ was employed.

The hardness (H_v) and fracture toughness (K_{IC}) were measured on the polished surfaces of the as-sintered samples to quantify the effect of TiO_2 addition on the room temperature mechanical properties of 8Y-CSZ. A Zwick microhardness tester (Zwick 3210) was employed for the measurements at a load of 5 kg for duration of 25 s. Ten tests were conducted for each composite. The hardness (H_v) was calculated using the following equation:

$$H_v = 1.854\,P/d^2 \tag{1}$$

where P is the applied load and d is the diagonal length of the indentation. The indentation fracture toughness (K_{IC}) was calculated using the equation proposed by Anstis et al. [14] (half-penny crack)

$$K_{IC} = 0.016(E/H_v)^{1/2}(P/a^{3/2}) \tag{2}$$

where E is elastic modulus and a is the crack length.

3. Results and discussion

3.1. XRD patterns

X-ray diffraction patterns of as-sintered samples are shown in Fig. 1 as a function of TiO_2 dopant concentration. When the dopant concentration is less than 5 wt%, only the cubic phase is present. When the dopant amount increases to 5 wt%, additional reflections from tetragonal phase zirconia start to appear and the c/a splitting becomes evident, especially at higher angle reflections such as (4 0 0) and (0 0 4) (Fig. 1(b)). Therefore, the addition of more than 5 wt% TiO_2 destabilizes the cubic phase and induces the formation of the tetragonal phase. However, even when the dopant amount was 10 wt%, only cubic and tetragonal zirconia were present and no TiO_2 or $TiZrO_4$ phases were observed. TiO_2 up to 10 wt% (corresponding to 15 mol%) could be accommodated in solid solution in the zirconia matrix, although tetravalent dopants smaller than zirconium ions usually do not form cubic zirconia solid solutions [15].

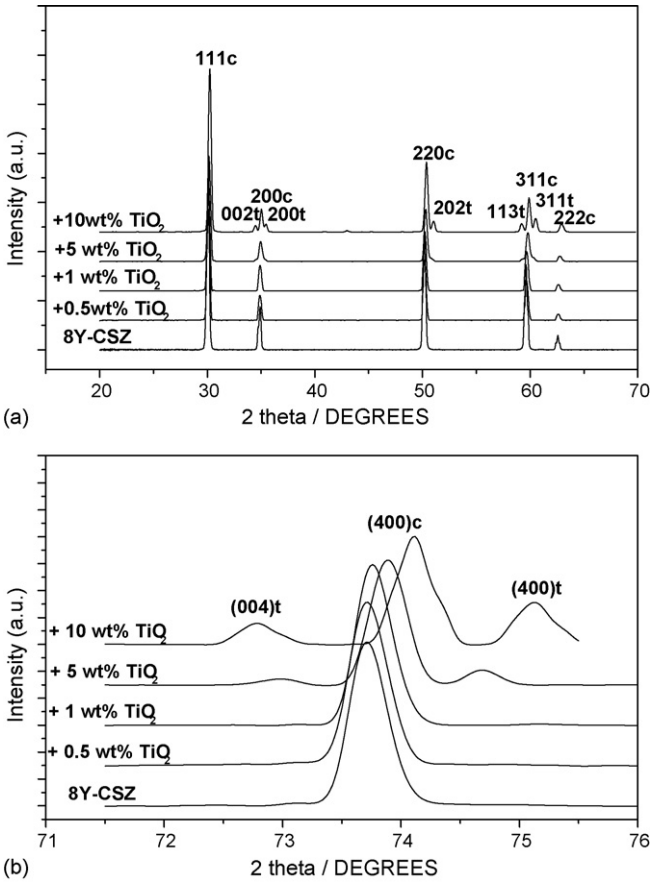

Fig. 1. X-ray diffraction patterns for undoped and TiO_2 doped 8Y-CSZ (a) 20–70° 2θ and (b) (4 0 0) peak splitting (c: cubic zirconia; t: tetragonal zirconia).

However in these samples, the XRD data indicate the existence of titania in solid solution and the decrease of the lattice parameter with increasing TiO_2 dopant up to 10 wt% TiO_2. The lattice parameters for undoped 8Y-CSZ and different amounts of TiO_2 doped 8Y-CSZ are listed in Table 1. The lattice decrease is due to the replacement of the Zr^{4+} ions (0.079 nm) by the smaller Ti^{4+} ions (0.068 nm).

The addition of 5 wt% or more TiO_2 to 8Y-CSZ induces the formation of tetragonal zirconia. The mole fraction for each phase can be calculated from Fig. 1(b) by the ratio [16]

$$\frac{M_c}{M_t} = 0.88\frac{I_c(400)}{I_t(400) + I_t(004)} \tag{3}$$

where M is the mole fraction, c cubic phase, t tetragonal phase, and I is the intensity. The mole percentage for cubic and tetragonal zirconia in the 5 wt% TiO_2 doped 8Y-CSZ was calculated to be 89 and 11%, respectively. When the dopant amount increased to 10 wt% TiO_2, the percentage of the tetragonal zirconia phase increased to 37%.

Table 1
Lattice parameters and phase constituents for TiO_2 doped 8Y-CSZ

TiO_2 (wt%)	0	0.1	0.3	0.7	1	5	10
a (cubic)	5.142	5.138	5.136	5.134	5.133	5.126	5.118
Phases present	c	c	c	c	c	89% c + 11% t	63% c + 37% t

Note: c: cubic zirconia, t: tetragonal zirconia.

3.2. SEM results

Typical SEM micrographs of as-sintered undoped and TiO_2 doped 8Y-CSZ samples are shown in Fig. 2. Fully densified bodies were obtained for 5 wt% TiO_2 doped 8Y-CSZ in contrast to 1 wt% TiO_2 doped 8Y-CSZ, which exhibited a small amount of intergranular porosity. The grain boundaries for the undoped sample were fairly regular. However, the 5 wt% TiO_2 doped samples developed more irregular grain boundaries with a large number of small grains present at grain junctions and grain boundaries, indicating that the grain growth of the large grains was inhibited by the small grains during sintering. EDS analysis indicated that the small grains were tetragonal zirconia (Y-TZP), consistent with the XRD patterns (Fig. 1). EDS analysis indicated that the yttria concentration in the small grains is much lower than that in large grains. Therefore, the small grains are the yttria deficient tetragonal phase and the large grains are the yttria rich cubic zirconia phase. In addition, the surface of the TiO_2 doped samples (Fig. 2(c)) is not as smooth as that in undoped one (Fig. 2(a)). Using EDS and XRD, Colomer and Jurado [17] found $TiZrO_4$ precipitates on the surface of cubic zirconia grains formed after severe thermal etching process. Not detectable in the bulk material by XRD, the possible appearance of $TiZrO_4$ seems to be a surface phenomenon.

The grain sizes and relative densities are plotted against TiO_2 concentration in Fig. 3. A comparison of the grain size of 8Y-CSZ samples with TiO_2 content shows that grain size increases with increasing TiO_2 content up to 1 wt% but further increases in TiO_2 result in a decreased grain size. The area fraction in Fig. 2(c) occupied by small grains with a grain size smaller than 1.2 μm is estimated to be 13%, which is close to the mole fraction of 11% tetragonal zirconia estimated from Eq. (3). Although a small addition of TiO_2 dopant promotes grain growth, density is the lowest in 1 wt% TiO_2-8Y-CSZ because of the porosity (Fig. 2(b)).

Grain size distributions for both undoped and 5 wt% TiO_2 doped 8Y-CSZ are shown in Fig. 4. The grain size distribution for undoped 8Y-CSZ is normal. However, a bimodal grain size distribution is observed for 5 wt% TiO_2 doped 8Y-CSZ. The bimodal grain size distribution is also evident in the micrograph Fig. 2(c). The average cubic grain size decreases with 5 wt% TiO_2 addition. Therefore, the addition of 5 wt% TiO_2 effectively limits the cubic grain growth by the pinning presence of small tetragonal grains. Yoshida et al. [11] reported that while 5 mol% TiO_2 (3.3 wt%) dopant nearly doubled the grain size compared to the undoped 8Y-CSZ, 10 mol% TiO_2 (6.7 wt%) doped specimens had the same grain size as undoped 8Y-CSZ and further addition of the dopant decreased the grain size. In their work, the XRD patterns for 5 mol% TiO_2 doped 8Y-CSZ indicated the presence of only single phase cubic zirconia. However, in the present work, 5 wt% TiO_2 (7.5 mol%) doped 8Y-CSZ clearly shows peaks from both tetragonal and cubic zirconia. Thus increasing grain growth with TiO_2 additions is effective only up to concentrations where the

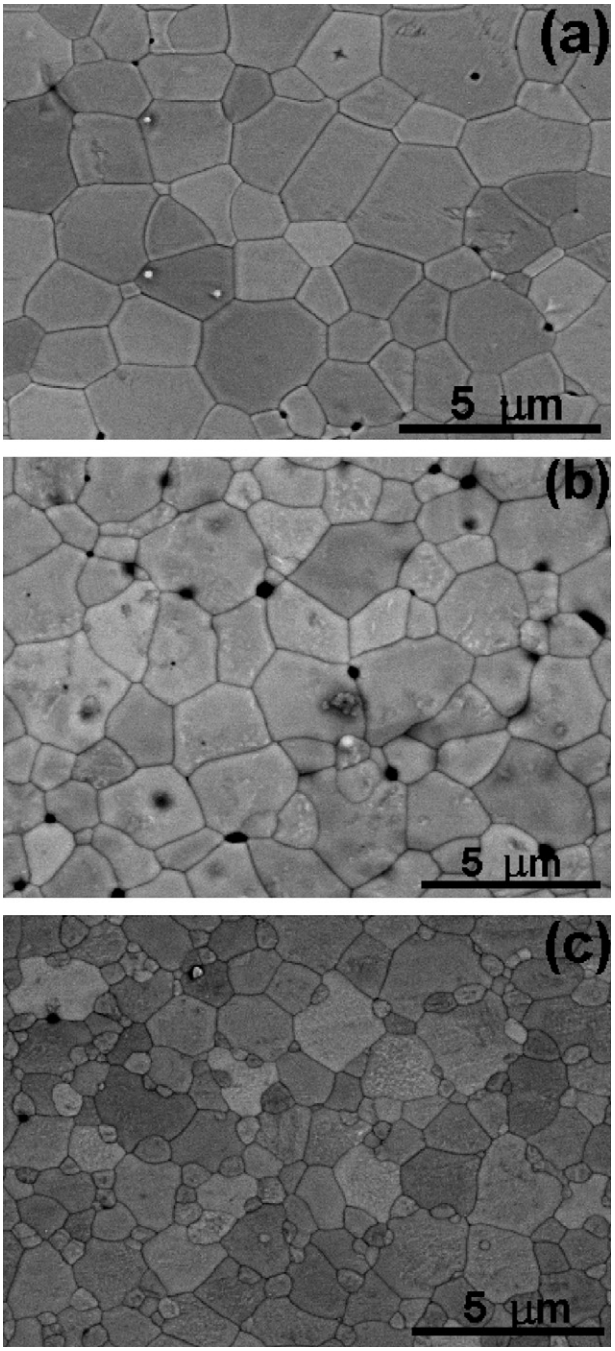

Fig. 2. SEM micrographs for: (a) undoped 8Y-CSZ, (b) 1 wt% TiO_2 doped 8Y-CSZ and (c) 5 wt% TiO_2 doped 8Y-CSZ.

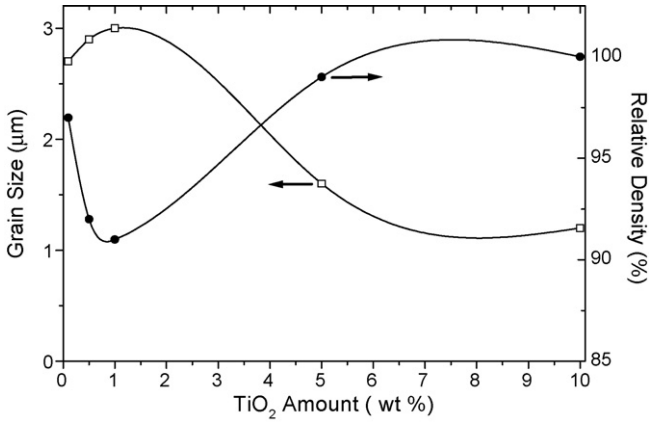

Fig. 3. The effect of TiO_2 dopant amount on the grain size and relative density after sintering.

tetragonal phase nucleates, between 5 and 7.5 mol% TiO_2 (i.e. 3.3–5 wt% TiO_2).

3.3. TEM results and EDS analysis

Typical TEM micrographs and EDS analyses for the as-sintered 10 wt% TiO_2 doped 8Y-CSZ samples are shown in Fig. 5. As seen in Fig. 5(a), the microstructure consists of both large and small grains. No glassy pockets were revealed at junctions using conventional transmission electron microscopy (Fig. 5(c)). In 10 wt% TiO_2 doped 8Y-CSZ samples, the grain shape is more irregular. Small grains at junctions and boundaries pin the grain boundaries of large grains, resulting in curved grain boundaries.

EDS analyses of both large and small grains are shown in Fig. 5(b). The EDS results show that both large and small grains contain Y, Zr, Ti and O. Therefore, the small grains are not TiO_2 precipitates but TiO_2 has been dissolved in the zirconia matrix. The solubility of Ti is different for the large and small grains, and correlates with the yttria concentration. The yttria concentration in large grains is double that in small grains, which is consistent with SEM-EDS results. The solubility of Ti in zirconia correlates with higher yttria concentration. Pyda and Haberko [18] and Lin et al. [19] found that the solubility of titania in TZP (3 mol% Y_2O_3) is about 14 mol%, while in YSZ it is 18 mol% at 1600 °C. The increase of Ti solubility in zirconia with yttria concentration also agrees with the phase relations in the ternary system ZrO_2–Y_2O_3–TiO_2 determined by Feighery et al. [20]. This is most probably because the increase of yttria concentration causes an increase in oxygen vacancies, thus enabling more Ti^{4+} ions to assume the preferred 6-fold coordination.

3.4. Room temperature mechanical properties

The results of room temperature mechanical property measurements are plotted in Fig. 6 for undoped and TiO_2 doped 8Y-CSZ samples. The addition of more than 5 wt% TiO_2 causes the formation of small tetragonal grains which help to limit the grain growth of the 8Y-CSZ matrix. However, as shown from Fig. 6, the hardness does not change significantly with changing TiO_2 dopant concentration and is maintained around 12 GPa. Similar hardness values for single phase 8Y-CSZ ceramics have been reported by Kwon et al. [5] and Tekeli [6]. Kwon et al. [5] also reported that the change in grain size did not affect the hardness of Al_2O_3 doped 8Y-CSZ composites.

In contrast, an increase of fracture toughness with increasing TiO_2 concentration is evident from Fig. 6. The fracture toughness values for undoped and 10 wt% TiO_2 doped 8Y-CSZ are 1.2 and 3.3 MPa $m^{1/2}$, respectively. Tekeli [6] has reported that the fracture toughness for undoped 8Y-CSZ is about 1.5 MPa $m^{1/2}$, while the addition of 10 wt% Al_2O_3 particles increased the fracture toughness to only 2.4 MPa $m^{1/2}$. The enhancement of fracture toughness due to TiO_2 additions can be explained by a change in the mode of fracture and the formation of tetragonal zirconia. Cracks in single cubic phase 8Y-CSZ ceramic propagate through the grains with a transgranular fracture mode [21] as observed in Fig. 7(a). However, the TiO_2 doped 8Y-CSZ (Fig. 7(b)) shows increased intergranular fracture at tetragonal zirconia/cubic zirconia interfaces and a more irregular crack path, compared to the straight transgranular crack path across

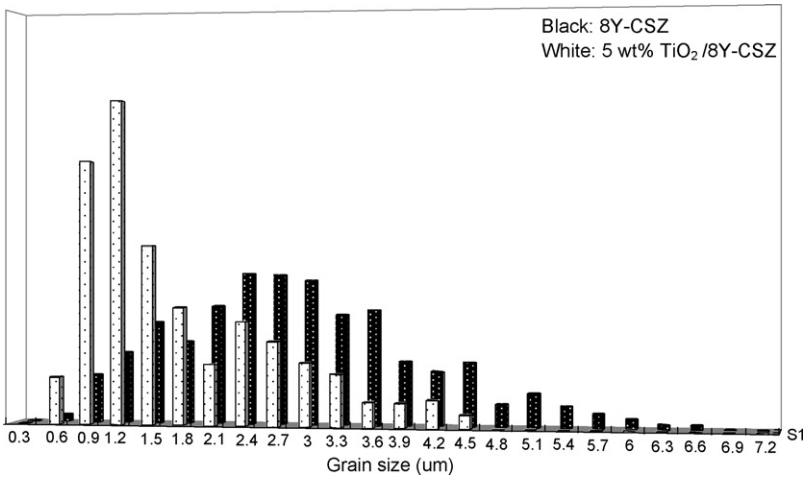

Fig. 4. Grain size distribution for undoped and 5 wt% TiO_2 doped 8Y-CSZ after sintering at 1450 °C for an hour.

cubic 8Y-CSZ grains (Fig. 7(a)). Transformation toughening due to the tetragonal to monoclinic phase transformation and the resultant volume expansion upon crack propagating will also cause an increase in toughness [22]. Follow the rule of mixture, the increased tetragonal content should also increase of fracture toughness for TiO_2 doped 8Y-CSZ at room temperature.

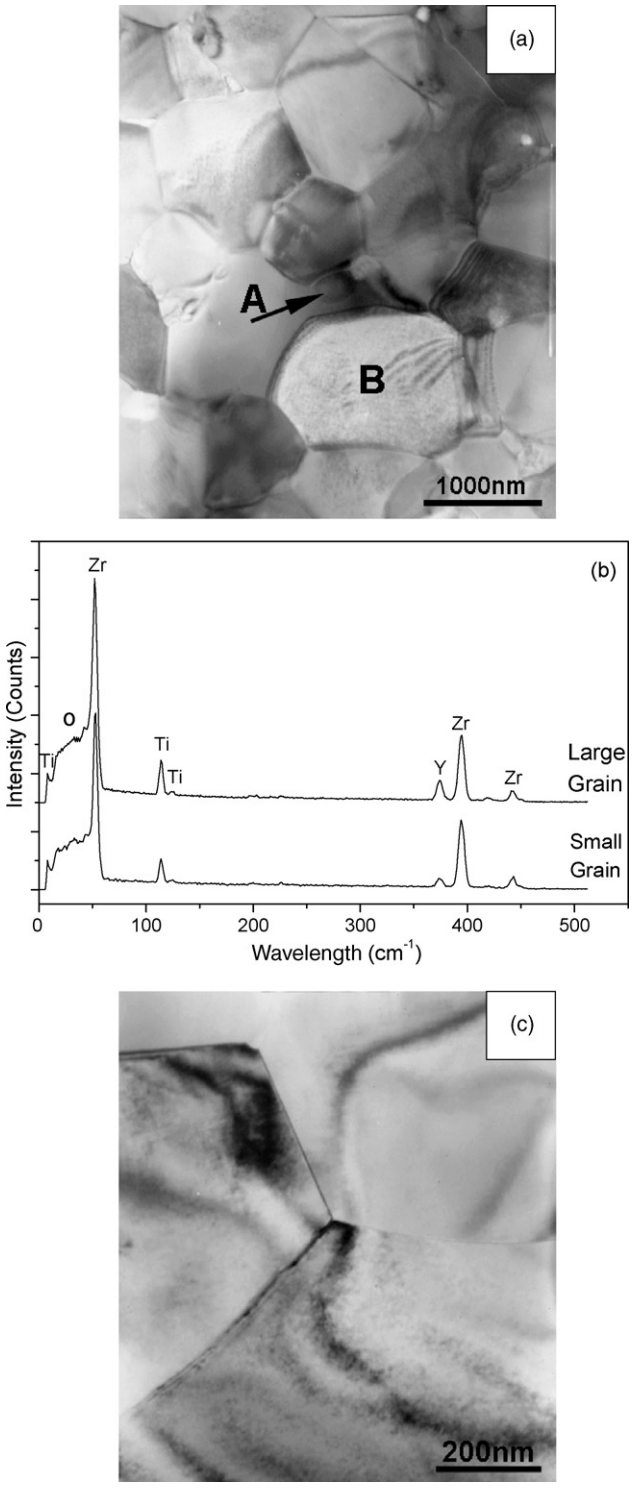

Fig. 5. Typical TEM micrographs for as-sintered 10 wt% TiO_2 doped 8Y-CSZ (a) small grains at junctions and boundaries, (b) EDS results for small grains (grain A) and large grains (grain B) and (c) sharp grain boundaries.

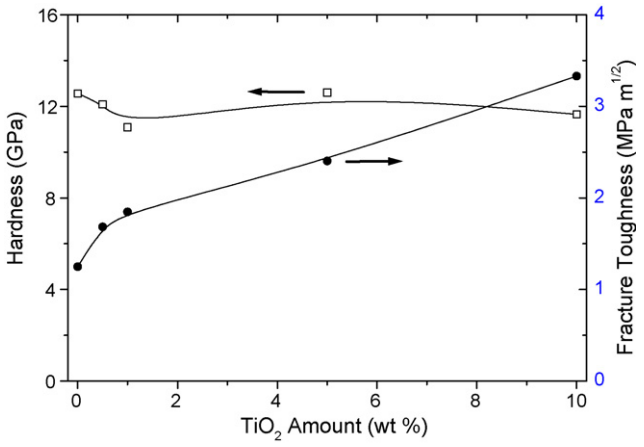

Fig. 6. The effect of TiO_2 content on the fracture toughness and hardness of 8Y-CSZ.

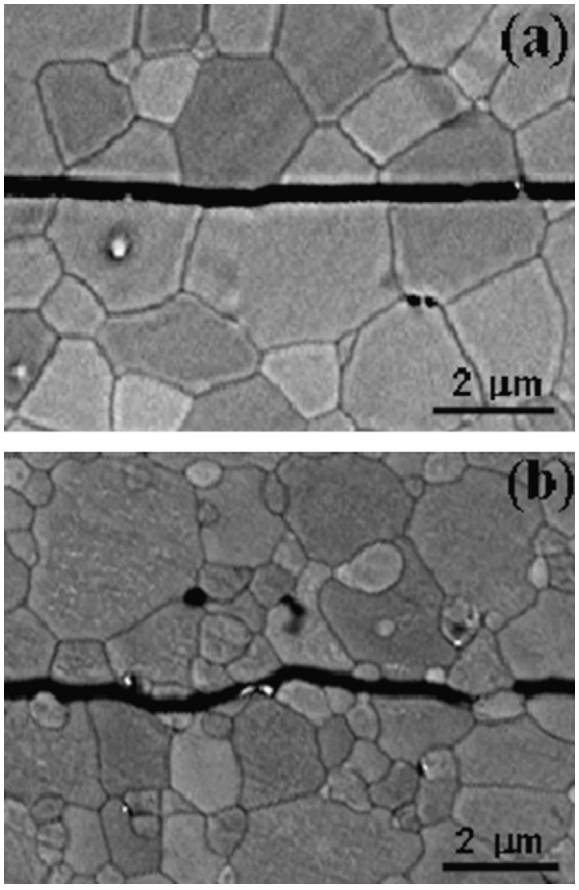

Fig. 7. Comparison of indentation crack paths in (a) undoped 8Y-CSZ and (b) 5 wt% TiO_2 doped 8Y-CSZ.

4. Conclusions

The phase evolution, microstructure and room temperature mechanical properties of TiO_2 doped 8Y-CSZ were investigated. 8Y-CSZ containing less than 5 wt% TiO_2 is single phase cubic zirconia. 8Y-CSZ containing 5–10 wt% TiO_2 consists of large cubic zirconia and small tetragonal zirconia grains with

TiO_2 in solid solution. Limited grain growth of cubic zirconia is due to the pinning effect from the formation of small tetragonal zirconia grains at boundaries and junctions. The solid solubility of TiO_2 in zirconia increased proportionally to the yttria concentration in solid solution. The hardness maintains a value of 12 GPa and does not change significantly with the TiO_2 dopant amount. However, the fracture toughness increases significantly with increasing dopant amounts due to a change in fracture mode and transformation toughening from tetragonal grains.

Acknowledgements

This research work is supported by DPT (the State Planning Organization of Turkey) under project number 2003K120470-18 and by the Division of Materials Research of the National Science Foundation (USA) under Grant No. 0207197.

References

[1] N.Q. Minh, J. Am. Ceram. Soc. 76 (1993) 563–588.
[2] R.A. Miller, Surf. Coat. Technol. 30 (1987) 1–11.
[3] T. Zhang, Z. Zeng, H. Huang, P. Hing, J. Kilner, Mater. Lett. 57 (2002) 124–129.
[4] K. Hiraga, K. Morita, B.N. Kim, Y. Sakka, Mater. Trans. 45 (2004) 3324–3329.
[5] N.H. Kwon, G.H. Kim, H.S. Song, H.L. Lee, Mater. Sci. Eng. A 299 (2001) 185–194.
[6] S. Tekeli, Compos. Sci. Technol. 65 (2005) 967–972.
[7] L.M. Navarro, P. Recio, J.R. Jurado, P. Duran, J. Mater. Sci. 30 (1995) 1949–1960.
[8] L. Donzel, S.G. Roberts, J. Eur. Ceram. Soc. 20 (2000) 2457–2462.
[9] M.F. Melo, J.S. Moya, P. Pena, S. De Aza, J. Mater. Sci. 20 (1985) 2711–2718.
[10] J.M. Bannister, J. Am. Ceram. Soc. 69 (1986) C-269–C-271.
[11] H. Yoshida, A. Kubo, H. Ito, Scripta Mater. 52 (2005) 365–368.
[12] N.P. Padture, M. Gell, E.H. Jordan, Science 296 (2002) 280–284.
[13] T. Lindegaard, C. Clausen, M. Mogensen, F.W. Poulsen, J.J. Bentzen, T. Jacobsen, E. Skou, M.J.L. Ostergard (Eds.), Fourteenth Riso International Symposium on Materials ScienceRiso National Laboratory, Roskilde, (1993), p. P311.
[14] G.R. Anstis, P. Chantikul, B.R. Lawn, D.B. Marshall, J. Am. Ceram. Soc. 64 (1981) 533–538.
[15] P. Li, I.W. Chen, J.E. Penner-Hahn, J. Am. Ceram. Soc. 77 (1994) 118–128.
[16] R.A. Miller, J.L. Smialek, R.G. Garlick, in: A.H. Heuer, L.W. Hobbs (Eds.), Advances in Ceramics, American Ceramic Society, Columbus, OH, 1981, pp. 291–353.
[17] M.T. Colomer, J.R. Jurado, J. Solid State Chem. 165 (2002) 79–88.
[18] W. Pyda, H. Haberko, Ceram. Int. 13 (1987) 113–118.
[19] C.L. Lin, D. Gan, P. Shen, Mater. Sci. Eng. A 129 (1990) 147–155.
[20] A.J. Feighery, J.T.S. Irvine, D.P. Fagg, A. Kaiser, J. Solid State Chem. 143 (1999) 273–276.
[21] P. Bhargava, B.R. Patternson, J. Am. Ceram. Soc. 80 (1997) 1863–1867.
[22] M. Rühle, A.G. Evans, Prog. Mater. Sci. 33 (1989) 85–167.